Applied Mathematics and Computation 219 (2013) 10044–10052

Contents lists available at SciVerse ScienceDirect

Applied Mathematics and Computation

journal homepage: www.elsevier.com/locate/amc

Numerical solution of transient heat conduction problems using improved meshless local Petrov–Galerkin method

Baodong Dai [a,*], Baojing Zheng [b], Qingxiang Liang [a], Linghui Wang [a]

[a] Department of Engineering Mechanics, Taiyuan University of Science & Technology, Taiyuan 030024, China
[b] School of Aeronautics and Astronautics, Dalian University of Technology, Dalian 116024, China

ARTICLE INFO

Keywords:
Meshless local Petrov–Galerkin method
Moving Kriging interpolation method
Heaviside step function
Transient heat conduction

ABSTRACT

An improved meshless local Petrov–Galerkin (MLPG) method is presented and applied to calculate the two-dimensional unsteady state heat conduction problems. In this method, the moving Kriging interpolation is employed instead of the traditional MLS approximation to construct the MLPG shape functions which possess Kronecker delta function property and thus make it easy to implement essential boundary conditions and then, the Heaviside step function is used as the test function over a local sub-domain. Since no mesh is needed either for integration of the local weak form, or for construction of the shape functions, the presently developed MLPG method is a truly meshless method. Several examples are performed to illustrate the accuracy and efficiency of the present method. A good agreement can be found among the proposed, analytical and finite element methods.

1. Introduction

Many engineering and science problems are associated with transient heat transfer problems and in such problems the temperature varies with respect to time, such as boilers, air-conditioning equipment and encapsulation. Therefore, the analysis of transient heat transfer is very important. These transient heat conduction problems are classically described by a partial differential equation associated with a set of boundary conditions and initial conditions. Analytical solutions to these boundary value and initial value problems are usually very limited. Over the past few decades, various numerical methods such as finite difference method (FDM), finite element method (FEM) and the boundary element method (BEM) have been well established and successfully applied to heat conduction problems [1]. Even though the methods mentioned above are very effective for these problems, they have been reported to have their own limits [2].

In recent years, meshless or element free methods have been developed as alternative numerical approaches in effort to eliminate known shortcomings of the mesh-based methods [3]. The main advantage of these methods is to approximate the unknown field by a linear combination of shape functions built without having recourse to a mesh of the domain. Instead, nodes are scattered in the domain and a certain weight function with a local support is associated with each of these nodes. Therefore, they are prime methods for certain class of problems such as crack propagation problems, dynamic impact problems, nonlinear thermal analysis and so on [4–7].

To date, some meshless methods have been applied to simulate transient heat conduction problems. The element-free Galerkin (EFG) method have been reported for solving composite heat transfer problems [8,9], unsteady and nonlinear heat transfer problems [10,11]. Cheng et al. used reproducing kernel particle method (RKPM) to analysis steady and unsteady heat conduction problems [12]. The MLPG method originated by Atluri and Zhu [13] has been successfully applied in heat

* Corresponding author.
E-mail address: Dai_baodong@126.com (B. Dai).

0096-3003/$ - see front matter © 2013 Elsevier Inc. All rights reserved.
http://dx.doi.org/10.1016/j.amc.2013.04.024

conduction problems [14–16]. Sladek et al. used the MLPG method to analyze transient heat conduction problems in non-homogeneous functionally graded materials (FGMs) [17]. Qian et al. analyzed transient heat conduction problems in a thick functionally graded plate by using MLPG method [18]. Peng and Cheng developed the boundary element-free method (BFEM) to analyze steady heat conduction problems [19]. Among all the meshless methods, the MLPG method has been widely used in solving heat conduction problems due to: (1). the use of local weak formulation of the problem; (2) no background mesh for integration of weak forms. However, there exists an inconvenience because of the difficulty in implementing some essential boundary conditions; the shape functions based on the MLS approximation lack the Kronecker's delta property [20].

In order to eliminate this shortcoming of the MLS shape functions, the moving Kriging interpolation technique, which has the Kronecker delta function and consistency property, can be employed instead of the traditional MLS approximation to construct the meshless shape functions. Gu has firstly proposed the moving Kriging interpolation and has successfully developed a new moving Kriging interpolation-based EFG for solving one-dimensional steady-state heat conduction problems [21]. Later, the meshless methods based on the moving Kriging interpolation have also been developed and studied, for example, the element-free Galerkin method using moving Kriging interpolation [22,23], the meshless local Kriging method [24–32], and the boundary node method based on the moving Kriging interpolation [33].

The present study is motivated by the promising applications of the moving Kriging interpolation in meshless methods and presents an improved MLPG method for transient heat conduction problems. This method uses the moving Kriging interpolation techniques to construct meshless shape functions for a set of randomly distributed points. The local weak form of partial differential equations (PDEs) is derived by the weighted residual formulation based on a simple shaped local domain. Additionally, in implementation of the local weak form, the Heaviside step function is used as the test function. In the end, three numerical examples will be shown to demonstrate the performance of the proposed method.

2. Moving Kriging shape function

2.1. Moving Kriging interpolation

Similar to the MLS approximation, the moving Kriging approach can be extended to any sub-domain $\Omega_x \subseteq \Omega$. From Ref. [21], the field variable $u(x)$ in the problem domain Ω can be approximated by $u^h(x)$. For any sub-domain, the local approximation can be defined as follows:

$$u^h(\boldsymbol{x}) = [\boldsymbol{p}^T(\boldsymbol{x})\mathbf{A} + \boldsymbol{r}^T(\boldsymbol{x})\mathbf{B}]\boldsymbol{u}, \tag{1}$$

or

$$u^h(\boldsymbol{x}) = \sum_k^n \phi_k(\boldsymbol{x}) u_k, \tag{2}$$

where the moving Kriging shape function $\phi_k(\boldsymbol{x})$ is defined by

$$\phi_k(x) = \sum_j^m p_j(\boldsymbol{x}) A_{jk} + \sum_i^n r_i B_{ik}, \tag{3}$$

matrixes $\mathbf{A}$ and $\mathbf{B}$ are known by the following equations

$$\mathbf{A} = (\mathbf{P}^T\mathbf{R}^{-1}\mathbf{P})^{-1}\mathbf{P}^T\mathbf{R}^{-1}, \tag{4}$$

and

$$\mathbf{B} = \mathbf{R}^{-1}(\mathbf{I} - \mathbf{P}\mathbf{A}), \tag{5}$$

where $\mathbf{I}$ is a unit matrix and vector $\boldsymbol{p}(\boldsymbol{x})$ is the polynomial with m basis functions

$$\boldsymbol{p}(\boldsymbol{x}) = \begin{Bmatrix} p_1(\boldsymbol{x}) \\ p_2(\boldsymbol{x}) \\ \vdots \\ p_m(\boldsymbol{x}) \end{Bmatrix}, \tag{6}$$

For the matrix $\boldsymbol{P}$ with size $n \times m$, values of the polynomial basis functions (6) at the given set of node are collected.

$$\boldsymbol{P} = \begin{bmatrix} p_1(\boldsymbol{x}_1) & p_2(\boldsymbol{x}_1) & \cdots & p_m(\boldsymbol{x}_1) \\ p_1(\boldsymbol{x}_2) & p_2(\boldsymbol{x}_2) & \cdots & p_m(\boldsymbol{x}_2) \\ \vdots & \vdots & \ddots & \vdots \\ p_1(\boldsymbol{x}_n) & p_2(\boldsymbol{x}_n) & \cdots & p_m(\boldsymbol{x}_n) \end{bmatrix}, \tag{7}$$

and vector $\boldsymbol{r}(\boldsymbol{x})$ in Eq. (1) is also given by

$$\boldsymbol{r}(\boldsymbol{x}) = \begin{Bmatrix} R(\boldsymbol{x}_1, \boldsymbol{x}) \\ R(\boldsymbol{x}_2, \boldsymbol{x}) \\ \vdots \\ R(\boldsymbol{x}_n, \boldsymbol{x}) \end{Bmatrix}. \tag{8}$$

$R(\boldsymbol{x}_i, \boldsymbol{x}_j)$ is the correlation function between any pair of nodes located at $\boldsymbol{x}_i$ and $\boldsymbol{x}_j$.

Many functions can be used as a correlation function $R(\boldsymbol{x}_i, \boldsymbol{x}_j)$, however, a simple and frequently used correlation function is the Gaussian function

$$R(\boldsymbol{x}_i, \boldsymbol{x}_j) = \exp\left(-\theta r_{ij}^2\right), \tag{9}$$

in which

$$r_{ij} = \left\|\boldsymbol{x}_i - \boldsymbol{x}_j\right\|, \tag{10}$$

and $\theta > 0$ represents a value of the correlation parameter used to fit the model. In addition, the correlation matrix $\mathbf{R}[R(\boldsymbol{x}_i, \boldsymbol{x}_j)]$ is also given in an explicit form

$$\mathbf{R}[R(\boldsymbol{x}_i, \boldsymbol{x}_j)] = \begin{bmatrix} 1 & R(\boldsymbol{x}_1, \boldsymbol{x}_2) & \cdots & R(\boldsymbol{x}_1, \boldsymbol{x}_n) \\ R(\boldsymbol{x}_2, \boldsymbol{x}_1) & 1 & \cdots & R(\boldsymbol{x}_2, \boldsymbol{x}_n) \\ \vdots & \vdots & \ddots & \vdots \\ R(\boldsymbol{x}_n, \boldsymbol{x}_1) & R(\boldsymbol{x}_n, \boldsymbol{x}_2) & \cdots & 1 \end{bmatrix}. \tag{11}$$

The partial derivatives of shape function can be easily obtained as

$$\phi_{k,x} = \frac{\partial \phi_k(\boldsymbol{x})}{\partial x} = \sum_j^m \frac{\partial p_j(\boldsymbol{x})}{\partial x} A_{jk} + \sum_i^n \frac{\partial r_i(\boldsymbol{x})}{\partial x} B_{ik}, \tag{12a}$$

$$\phi_{k,y} = \frac{\partial \phi_k(\boldsymbol{x})}{\partial y} = \sum_j^m \frac{\partial p_j(\boldsymbol{x})}{\partial y} A_{jk} + \sum_i^n \frac{\partial r_i(\boldsymbol{x})}{\partial y} B_{ik}. \tag{12b}$$

2.2. Correlation parameter θ vs. shape functions

The effect of the correlation parameter θ vs. the shape functions is studied in this section. Considering a support domain $\Omega = [0, 1]$ in one dimension with five uniformly distributed points of [0, 0.25, 0.5, 0.75, 1]. The values of the shape functions and the first-order derivatives, which are evaluated at $x = 0.5$ using several typical chosen values of correlation factor on a bound of 0.1–500, is shown in Fig. 1.

Obviously, the quality of the shape function is heavily influenced by the correlation parameter θ. In order to get 'optimal' θ for meshless method, in our study, we found that the 'optimal' θ is dependent on the number of nodes in the compact support, empirical formula is obtained as

$$\theta = \omega / h^2, \tag{13}$$

where ω is a constant, h is the average distance of the nodes in the support domain. It is a good choice to take $\omega = 0.03 - 0.2$. In this paper, $\omega = 0.1$ is studied.

2.3. Desirable properties of moving Kriging interpolation

It can be found from the Fig. 1(a) that the shape functions possess the delta function property, namely

$$\phi_k(\boldsymbol{x}_j) = \begin{cases} 1 & (k = j; k, j = 1, 2, \ldots, n) \\ 0 & (k \neq j; k, j = 1, 2, \ldots, n) \end{cases}. \tag{14}$$

The other important property of the moving Kriging shape functions is the consistency property [21]

$$\sum_{k=1}^n \phi_k(\boldsymbol{x}) = 1, \tag{15a}$$

$$\sum_{k=1}^n \phi_k(\boldsymbol{x}) x_k = x. \tag{15b}$$

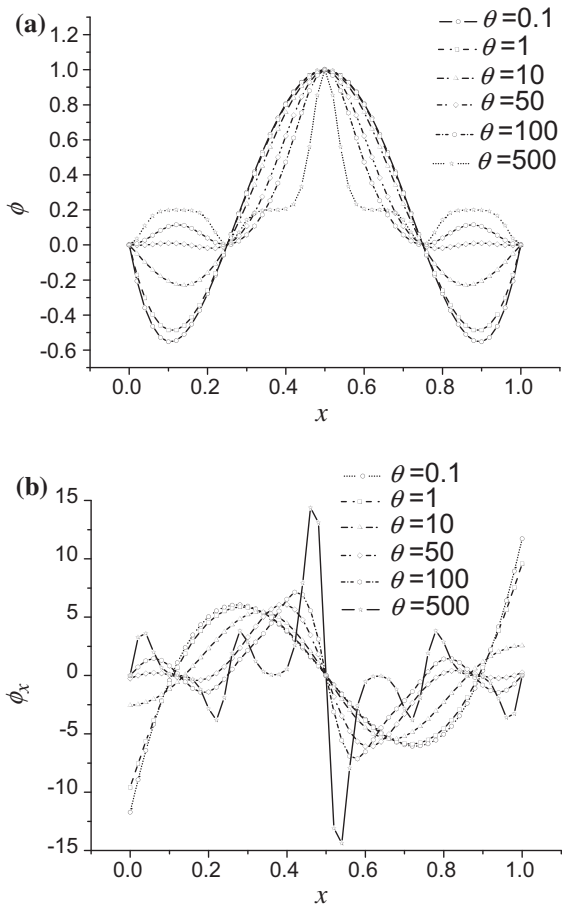

Fig. 1. The quality of (a) shape functions and (b) first-order derivatives of the shape function.

3. The MLPG formulation of transient heat conduction

Consider a two-dimensional transient heat conduction problem for a stationary medium on a domain Ω bounded by Γ, the governing equation is

$$\rho c \frac{\partial T}{\partial t} = \frac{\partial}{\partial x}\left(k_x \frac{\partial T}{\partial x}\right) + \frac{\partial}{\partial y}\left(k_y \frac{\partial T}{\partial y}\right) + Q, \tag{16}$$

where $T(x, y, t)$ is the temperature field, t is time, ρ is the density of material, c is the specific heat, k_x and k_y are the thermal conductivities in the x- and y-directions, respectively, Q is the heat generation per unit volume. The initial conditions and the boundary conditions of the problem are

$$T(x, y, 0) = T_0 \quad \text{in } \Omega, \tag{17a}$$

$$T = \bar{T} \quad \text{on } \Gamma_1, \tag{17b}$$

$$k_x \frac{\partial T}{\partial x} n_x + k_y \frac{\partial T}{\partial y} n_y = q \quad \text{on } \Gamma_2, \tag{17c}$$

$$k_x \frac{\partial T}{\partial x} n_x + k_y \frac{\partial T}{\partial y} n_y = h(T_a - T) \quad \text{on } \Gamma_3, \tag{17d}$$

where Γ_1, Γ_2 and Γ_3 are the Dirichlet boundary, the Neumann boundary and the Robin boundary, respectively. n_x and n_y are direction cosines, h is the heat transfer coefficient, T_a is the surrounding medium temperature and q is the boundary heat flux.

The local weak form is constructed over a sub-domain Ω_s bounded by Γ_s. The local sub-domains overlap each other, and cover the whole problem domain Ω. They could be of any geometric shape and size. For simplicity, they are taken to be of circular shape or rectangular shape. Using the local weighted residual method, the generalized local weak form of Eq. (16) can be written as

$$\int_{\Omega_s} w\left[\rho c\frac{\partial T}{\partial t}-\frac{\partial}{\partial x}\left(k_x\frac{\partial T}{\partial x}\right)-\frac{\partial}{\partial y}\left(k_y\frac{\partial T}{\partial y}\right)-Q\right]\mathrm{d}\Omega=0, \tag{18}$$

where w is the test function.

Using the divergence theorem in Eq. (18), the following form can be obtained as

$$\int_{\Omega_s} w\left(\rho c\frac{\partial T}{\partial t}-Q\right)d\Omega+\int_{\Omega_s}\left(k_x\frac{\partial T}{\partial x}\frac{\partial w}{\partial x}+k_y\frac{\partial T}{\partial y}\frac{\partial w}{\partial y}\right)d\Omega-\int_{\Gamma_s} w\left(k_x\frac{\partial T}{\partial x}n_x+k_y\frac{\partial T}{\partial y}n_y\right)d\Gamma=0. \tag{19}$$

In order to simplify Eq. (19), the test function w is chosen such that they eliminate or simplify the domain integral on Ω_s. This can be accomplished by using the Heaviside step function

$$w=\begin{cases}1, & \boldsymbol{x}\in\Omega_s\\ 0, & \boldsymbol{x}\notin\Omega_s\end{cases}. \tag{20}$$

Using the Heaviside step function as the test function and the natural boundary condition defined by Eq. (17), the local weak form (19) can be rewritten as

$$\int_{\Omega_s}\rho c\frac{\partial T}{\partial t}d\Omega+\int_{\Gamma_{s3}} hT d\Gamma=\int_{\Omega_s} Q d\Omega+\int_{\Gamma_{s1}} q d\Gamma+\int_{\Gamma_{s2}} q d\Gamma+\int_{\Gamma_{s3}} hT_a d\Gamma, \tag{21}$$

where Γ_{s1} is a part of the local boundary Ω_s over which no boundary conditions are specified, Γ_{s2} is the intersection of Γ_2 and the boundary Γ_s, Γ_{s3} is the intersection of Γ_3 and the boundary Γ_s.

In the transient heat conduction, temperature T is a function of both the spatial coordinates and time. It can be rewritten as

$$T(\boldsymbol{x},t)=\sum_k^n \phi_k(\boldsymbol{x})T_k(t). \tag{22}$$

Substituting the temperature expression in Eq. (22) into the local weak form (21), the discrete equation for all nodes is given as

$$\boldsymbol{C}\dot{\boldsymbol{T}}(t)+\mathbf{K}\boldsymbol{T}(t)=\boldsymbol{P}(t), \tag{23}$$

in which

$$\mathbf{C}_{IJ}=\int_{\Omega_s}\rho c\phi_J d\Omega, \tag{24}$$

$$\mathbf{K}_{IJ}=\int_{\Gamma_3} h\phi_J d\Gamma, \tag{25}$$

$$\mathbf{P}(t)_I=\int_{\Omega_s} Q d\Omega+\int_{\Gamma_2} q d\Gamma+\int_{\Gamma_3} hT_a d\Gamma. \tag{26}$$

Using backward difference technique for time approximation, for any time step, Eq. (23) can be written as

$$\left(\mathbf{C}+\frac{1}{2}\mathbf{K}\Delta t\right)\boldsymbol{T}_{n+1}=\mathbf{P}\Delta t+\left(\mathbf{C}-\frac{1}{2}\mathbf{K}\Delta t\right)\boldsymbol{T}_n. \tag{27}$$

4. Numerical examples

4.1. Dirichlet problem of a square domain

In order to investigate the accuracy of the present method, we consider the transient heat conduction problem in a square domain $L\times L$ with the Dirichlet boundary conditions on all the sides. The basic parameters used in the computation are length of each edge $L=\pi$ mm, mass density $\rho=10^3$ kg/m^3, specific heat $c=10^3$ J/(kg$\cdot^\circ$C), thermal conductivities $k_x=k_y=10^3$ W/(m$\cdot^\circ$C). The Dirichlet boundary conditions are assumed to be zero. The initial temperature on all the sides are assumed as

$$T(x,y,0)=10\sin(x)\sin(y),$$

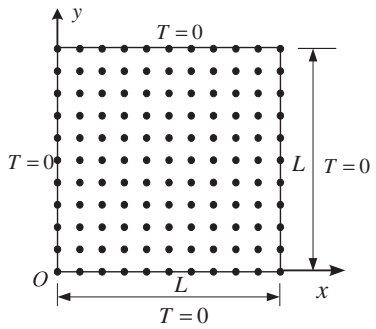

Fig. 2. The nodal arrangement.

the exact solution is given as follows:

$$T(x,y,t) = 10\sin(x)\sin(y)e^{-2t}.$$

As shown in Fig. 2 and 121 uniformed nodes are used to discretize the problem domain. In the computation, the parameters of the influence domain and sub-domain are taken as $\alpha = 4.0$ and $\beta = 0.5$, respectively. We have used the length of the time steps $\Delta t = 0.02$ s. The comparison of the numerical results obtained by the present method with the exact solution of the temperature at $y = \pi/2$ is shown in Fig. 3 at different times. Fig. 4 shows the comparison of numerically computed time evolution of the temperature at two points A $(\pi/4, \pi/4)$ and B $(\pi/2, \pi/2)$ with the exact solutions. It can be seen that the results obtained by the present method have a good agreement with the exact solutions.

4.2. Mixed problem of a square domain

In this example, the transient heat conduction problem is considered in the square domain as in the previous example ($L = 100$ mm). The basic parameters taken in the computation are mass density $\rho = 10^3$ kg/m^3, specific heat

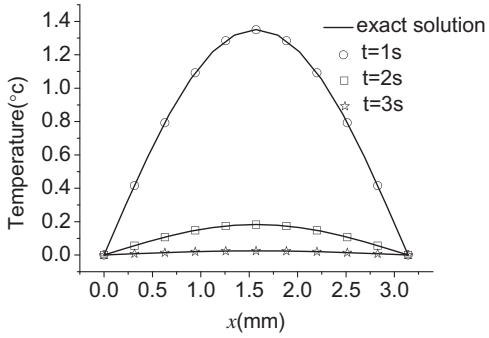

Fig. 3. Comparison of temperature distributions at $y = \pi/2$ along x axe.

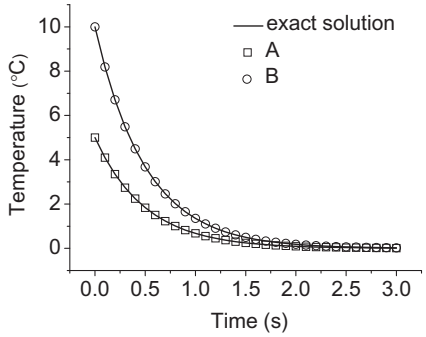

Fig. 4. Temperature evolution at points A $(\pi/4, \pi/4)$ and B $(\pi/2, \pi/2)$.

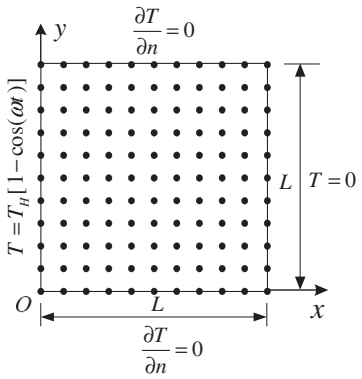

Fig. 5. Geometry and discretization of the square domain with time-dependent Dirichlet boundary condition.

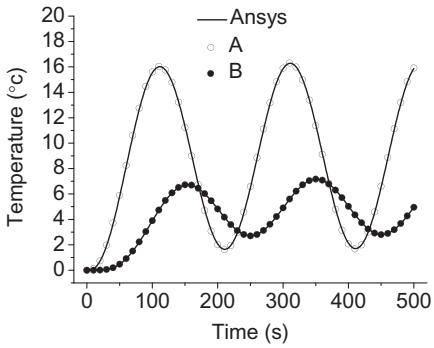

Fig. 6. Temperature evolution at points A (10, 50) and B (50, 50).

$c = 10^3$ J/(kg $\cdot^\circ$ C), thermal conductivities $k_x = k_y = 1.6 \times 10^4$ W/(m $\cdot^\circ$ C). The initial temperature is assumed to be zero. The top and bottom of the square domain are thermally insulated and the Dirichlet boundary conditions are assumed on the lateral sides at $t > 0$ as

$$T(100, y, t) = 0^\circ\mathrm{C},$$

$$T(0, y, t) = T_H[1 - \cos(\omega t)],$$

where $T_H = 10\ ^\circ$C, $\omega = \pi/100$ rad/s.

The discretization of the problem domain with 121 nodes is shown in Fig. 5. In the computation, the parameters of the influence domain and sub-domain are taken as $\alpha = 4.0$ and $\beta = 0.5$, respectively. We have used the length of the time steps $\Delta t = 0.125$ s. The comparison of the numerical results obtained by the present method and the finite element method (Ansys soft) is shown in Fig. 6, where the time evolution of the temperature at two points A (10, 50) and B (50, 50)is presented.

4.3. Mixed problem of a rectangular prism

In the last example, the transient heat conduction problem with heat exchange is considered in the rectangular prism domain $2L \times L$ ($L = 10$ mm). The initial temperature is assumed to be 20 °C. The top and bottom of the rectangular domain are thermally insulated, the external temperatures of the left and the right edges are assumed to be 100 °C. The basic parameters taken in the computation are mass density $\rho = 10^3$ kg/m^3, specific heat $c = 10^3$ J/(kg °C), heat transfer coefficient $h = 1600$ W/(m^2 $\cdot^\circ$ C), thermal conductivities $k_x = k_y = 16$ W/(m $\cdot^\circ$ C)

231 uniformed nodes are used to discretize the problem domain, as in Fig. 7. In the computation, the parameters of the influence domain and sub-domain are taken as $\alpha = 4.0$ and $\beta = 0.5$, respectively. We have used the length of the time steps $\Delta t = 0.01$ s. Table 1 shows the comparison of numerically computed the values of the temperature at three points A (0, 0), B (5, 5) and C (10, 0) with the exact solutions at different times. It can be seen that the results obtained by the present method is better than the FEM's [34].

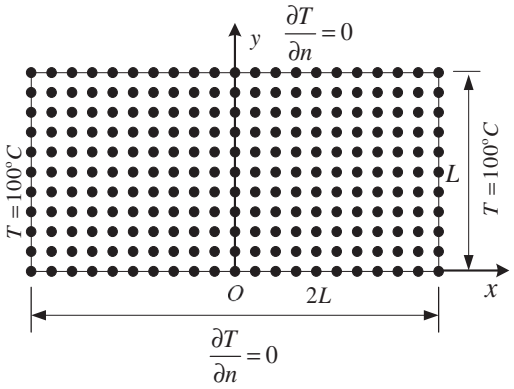

Fig. 7. Geometry and discretization of the rectangular prism domain.

Table 1
The temperature and relative error by the present method and FEM.

Time	Node	Exact	Present		FEM	
			Temperature	Error (%)	Temperature	Error (%)
1.0	A	22.304	22.330	0.117	21.340	4.32
	B	27.456	27.474	0.066	26.342	4.06
	C	46.384	46.369	0.032	45.236	2.47
2.0	A	29.344	29.446	0.348	28.261	3.69
	B	35.776	35.768	0.022	34.641	3.17
	C	53.928	53.894	0.063	52.934	1.84
3.0	A	37.232	37.307	0.201	36.162	2.87
	B	42.944	42.974	0.070	41.849	2.55
	C	59.072	59.048	0.041	58.271	1.36

5. Conclusions

A new formulation of improved MLPG method has been successfully applied to the transient heat conduction problems in this paper. The main attractive feature of the proposed approach is in the use of the moving Kriging interpolation as the trail function, therefore, the essential boundary conditions can be enforced as the FEM, and the Heaviside step function as the test function of the local weighted residual method, it does not involve any domain integral for constructing the stiffness matrix. Some test problems were studied by the proposed scheme and compared with analytical solutions and FEM. It is shown that the results are complete agreement and the proposed solution technique is quite efficient.

References

[1] W.J. Minkowycz, E.M. Sparrow, G.E. Schneider, R.H. Pletcher, Handbook of Numerical Heat Transfer, John Wiley and Sons, Inc., New York, 1988.
[2] S.J. Owen, A survey of unstructured mesh generation technology, in: Proceedings of Seventh International Meshing Round Table, Sandia National Laboratories, 1998, pp. 239–267.
[3] T. Belytschko, Y. Krongauz, D. Organ, M. Fleming, P. Krysl, Meshless methods: an overview and recent developments, Comput. Methods Appl. Mech. Eng. 139 (1996) 3–47.
[4] T. Belytschko, Y.Y. Lu, L. Gu, Element-free Galerkin methods, Int. J. Numer. Meth. Eng. 37 (1994) 229–256.
[5] L. Chen, Y.M. Cheng, The complex variable reproducing kernel particle method for two-dimensional elastodynamic, Chin. Phys. B 19 (2010) 090204.
[6] W.K. Liu, Y.J. Chen, Wavelet and multiple scale reproducing kernel methods, Int. J. Numer. Meth. Fluids 21 (1995) 901–931.
[7] Y.M. Cheng, M.J. Peng, Boundary element-free method for elastodynamics, Sci. China Ser. G Phys. Mech. Astron. 48 (2005) 641–657.
[8] I.V. Singh, A numerical solution of composite heat transfer problems using meshless method, Int. J. Heat Mass Transfer 47 (2004) 2123–2138.
[9] I.V. Singh, M. Tanaka, Heat transfer analysis of composite slabs using meshless element free Galerkin method, Comput. Mech. 38 (2006) 521–532.
[10] A. Singh, I.V. Singh, R. Prakash, Meshless analysis of unsteady-state heat transfer in semi-infinite solid with temperature-dependent thermal conductivity, Int. J. Heat Mass Transfer 33 (2006) 231–239.
[11] A. Singh, I.V. Singh, R. Prakash, Numerical solution of temperature-dependent thermal conductivity problems using a meshless method, Numer. Heat Transfer Part A 50 (2006) 125–145.
[12] R.J. Cheng, K.M. Liew, The reproducing kernel particle method for two-dimensional unsteady heat conduction problems, Comput. Mech. 45 (2009) 1–10.
[13] S.N. Atluri, T. Zhu, A new meshless local Petrov–Galerkin (MLPG) approach in computational mechanics, Comput. Mech. 22 (1998) 17–27.
[14] L.H. Liu, Meshless method for radiation heat transfer in graded index medium, Int. J. Heat Mass Transfer 49 (2006) 219–229.
[15] X.H. Wu, W.Q. Tao, Meshless method based on the local weak-forms for steady-state heat conduction problems, Int. J. Heat Mass Transfer 51 (2008) 3103–3112.
[16] Q.H. Li, S.S. Chen, G.X. Kou, Transient heat conduction analysis using the MLPG method and modified precise time step integration method, J. Comput. Phys. 230 (2011) 2736–2750.

[17] J. Sladek, V. Sladek, S.N. Atluri, Meshless local Petrov–Galerkin method for heat conduction problems in an anisotropic medium, CMES-Comput. Model. Eng. Sci. 6 (2004) 309–318.
[18] L.F. Qian, R.C. Batra, Three-dimensional transient heat conduction in a functionally graded thick plate with a higher-order plate theory and a meshless local Petrov–Galerkin method, Comput. Mech. 35 (2005) 214–226.
[19] M.J. Peng, Y.M. Cheng, A boundary element-free method (BEFM) for two-dimensional potential problems, Eng. Anal. Bound. Elem. 33 (2009) 77–82.
[20] P. Lancaster, K. Salkauskas, Surface generated by moving least squares method, Math. Comput. 37 (1981) 141–158.
[21] L. Gu, Moving Kriging interpolation and element-free Galerkin method, Int. J Numer. Meth. Eng. 56 (2003) 1–11.
[22] P. Tongsuk, W. Kanok-Nukulchai, Further investigation of element-free Galerkin method using moving Kriging interpolation, Int. J. Comput. Meth. 1 (2004) 345–364.
[23] T.Q. Bui, M. Ngoc Nguyen, C. Zhang, A moving Kriging interpolation-based element-free Galerkin method for structural dynamic analysis, Comput. Method Appl. Mech. Eng. 200 (2011) 1354–1366.
[24] T.Q. Bui, N.T. Nguyen, H. Nguyen-Dang, A moving Kriging interpolation-based meshless method for numerical simulation of Kirchhoff plate problems, Int. J. Numer. Meth. Eng. 77 (2009) 1371–1395.
[25] P. Zhu, K.M. Liew, Free vibration analysis of moderately thick functionally graded plates by local Kriging meshless method, Compos. Struct. 93 (2011) 2925–2944.
[26] V. Sayakoummane, W. Kanok-Nukulchai, A meshless analysis of shells based on moving Kriging interpolation, Int. J. Comput. Meth. 4 (2007) 543–565.
[27] K.Y. Lam, Q.X. Wang, H. Li, A novel meshless approach-local Kriging (LoKriging) method with two-dimensional structural analysis, Comput. Mech. 33 (2004) 235–244.
[28] Y.T. Gu, Q.X. Wang, K.Y. Lam, A meshless local Kriging method for large deformation analysis, Comput. Meth. Appl. Mech. Eng. 196 (2007) 1673–1684.
[29] K.Y. Dai, G.R. Liu, K.M. Lim, Y.T. Gu, Comparison between the radial point interpolation and the Kriging interpolation used in meshfree methods, Comput. Mech. 32 (2003) 60–70.
[30] H. Li, Q.X. Wang, K.Y. Lam, Development of a novel meshless Local Kriging (LoKriging) method for structural dynamic analysis, Comput. Meth. Appl. Mech. Eng. 193 (2004) 2599–2619.
[31] B.J. Zheng, B.D. Dai, Improved meshless local Petrov–Galerkin method for two-dimensional potential problems, Acta Phys. Sin. 59 (2010) 5182–5189 (in Chinese).
[32] B.J. Zheng, B.D. Dai, A meshless local moving Kriging method for two-dimensional solids, Appl. Math. Comput. 218 (2011) 563–573.
[33] X.G. Li, B.D. Dai, L.H. Wang, A moving Kriging interpolation-based boundary node method for two-dimensional potential problems, Chin. Phys. B 19 (2010) 12020.
[34] L. Chen, Y.M. Cheng, The complex variable reproducing kernel particle method for transient heat conduction problems, Acta Phys. Sin. 10 (2008) 6047–6055 (in Chinese).